DETECTION OF A SATELLITE ORBITING THE NUCLEUS OF COMET HALE–BOPP (C/1995 O1) *

Z. SEKANINA
Jet Propulsion Laboratory, California Institute of Technology, Pasadena, CA, USA

(Received 4 February 1998; Accepted 14 December 1998)

Abstract. This paper reports on the detection of a satellite around the principal nucleus of comet Hale–Bopp. As shown elsewhere, a successful morphological model for the comet's dust coma necessitates the postulation of overlapping jet activity from a comet pair. The satellite has been detected digitally on images taken with the Hubble Space Telescope's Wide Field Planetary Camera 2 in the planetary mode on five days in May–October 1996. An average satellite-to-primary signal ratio is 0.21 ± 0.03, which implies that the satellite is $\sim$30 km in diameter, assuming the main nucleus is $\sim$70 km across. To avoid collision, the separation distance must exceed 50–60 km at all times. The satellite's projected distances on the images vary from 160 to 210 km, or 0.06 to 0.10 arcsec. The satellite was not detected in October 1995, presumably because of its subpixel separation from the primary. The radius of the gravitational sphere of action of the principal nucleus 70 km in diameter is 370–540 km at perihelion, increasing linearly with the Sun's distance: the satellite appears to be in a fairly stable orbit. Its orbital period at $\sim$180 km is expected to be $\sim$2–3 days, much shorter than the intervals between the HST observations. If the main nucleus should be no more than 42 km across, Weaver et al.'s upper limit, the satellite's orbit could become unstable, with the object drifting away from the main nucleus after perihelion. Potentially relevant ground-based detections of close companions are reported. Efforts to determine the satellite's orbit and the total mass of the system will get under way in the near future.

Keywords: Comet Hale–Bopp, orbiting satellite, nuclear size, sphere of action

1. Introduction

Even though comet Hale–Bopp is unquestionably one of the most spectacular comets ever observed, reports of wide, easily detectable nuclear multiplicity are conspicuously absent. Because of usual difficulties with recognizing *close* nuclear companions, it is prudent to examine this issue on data of the highest available spatial resolution. Luckily, images were taken with the planetary mode (0.0455 arcsec/pixel) charge coupled device (CCD) of the Hubble Space Telescope's (HST) Wide-Field Planetary Camera 2 (WFPC-2) through an F675W filter; they have kindly been provided to me by H. A. Weaver.

Reported in the following are the results of my computer analysis of the near-nucleus region on the HST images that were taken on six dates between October 23,

Earth, Moon and Planets **77:** 155–163, 1997–1999.

1995 and October 17, 1996. The circumstances of these observations are presented in Table I of Sekanina (1997–1999). The near-nucleus signal distribution has been modelled in fields of 15 pixels, or nearly 0.7 arcsec, across and centered on the pixel of peak brightness. Each of these fields consists of 157 pixels. The modelling procedure is based on an iterative least-squares differential-correction technique, which was described in detail in Sekanina (1995) and has been upgraded since (Sekanina, 1997–1999). Its purpose is twofold. One, it allows the user to deconvolve the contributions from the nucleus and from the coma and thereby to extract the integrated signal of the nucleus. Two, it offers a convenient tool for detecting additional objects as secondary point sources in immediate proximity to the nucleus. It is in this capacity that the procedure has been employed in the present investigation.

2. Detection and the Results

When the observed signal distribution was interpreted to be due entirely to the dust coma, no converging solution could be derived for images on any of the six dates, indicating the presence of a sizable nucleus at the peak-signal location. Unexpectedly, the optimized solutions that accounted for a coma and a single nucleus failed to offer a satisfactory distribution of signal residuals. With the observed coma profile approximated by an anisotropic law of type A (cf. Equation (3) of Sekanina (1997–1999)), the solution to this problem is exemplified on the image of July 25, 1996 in Table I. In a right-handed coordinate system, each pixel $\{X, Y\}$, subtending 90.4 km at the comet, is defined by X increasing down and Y increasing to the right. The field of 157 pixels with signal residuals is centered on the peak-signal pixel {10, 10}. The north direction is to the upper right, making an angle of 23° with the $-X$ axis and 67° with the $+Y$ axis. East is 90° *clockwise* from the north.

The distribution of signal residuals, after the contributions from the dust coma and the principal nucleus have been accounted for, is shown in the upper panel of Table I. The pixel coordinates of the nucleus are derived to be $X = 10.41 \pm 0.01$ and $Y = 9.56 \pm 0.01$ (formal errors). A prominent clump of positive residuals (enclosed in a box), with a maximum excess signal of +180 ADU (CCD analog-to-digital intensity units per pixel^2) in pixel {9, 10}, is encircled by a ring of distinctly negative residuals, with an extreme signal of −108 ADU in pixel {10, 11}. The total amplitude of 288 ADU contrasts with an expected noise of only about ±15 ADU in the critical pixels, suggesting a huge effect. Also present is some systematic trend across the field, from predominantly negative residuals on the left to mostly positive ones on the right. It is noticed that this uneven distribution of residuals does not follow the general pattern of surface brightness, with the coma being the most prominent in the northerly direction.

Perplexities of this kind are formerly recognized signatures of a neglected point source that is situated near the clump's peak (Sekanina, 1995). Indeed, introducing

TABLE I

Pixel-signal residuals, observed minus modelled (in ADU), for the July 25, 1996 image of comet Hale–Bopp from the solutions involving one (top) and nine (bottom) point sources

X (pixels)	*Y* (pixels) 3	4	5	6	7	8	9	10	11	12	13	14	15	16	17	*X* (pixels)
3							+3	+28	+39							3
4					−12	−5	+7	+10	+12	+40	+70					4
5				−19	−24	−14	−6	−17	−30	+6	+44	+77				5
6			−20	−25	−31	−4	−7	−26	−70	−26	+10	+42	+73			6
7		−12	−25	−30	−35	−13	+24	−5	−67	−54	−11	+29	+50	+59		7
8		−16	−26	−35	−37	+8	+91	+102	+4	−54	−25	+4	+35	+49		8
9	−14	−22	−35	−47	−10	+91	+57	+180	+99	−44	−39	−16	+23	+41	+62	9
10	−8	−21	−32	−36	−4	−62	−66	+3	−108	−67	−51	−19	+19	+39	+61	10
11	−8	−23	−33	−33	−14	−46	+73	−12	−103	−24	−55	−15	+26	+47	+59	11
12		−20	−28	−35	−30	+68	−16	+4	+96	−13	−27	−8	+26	+45		12
13		−16	−29	−39	−45	−6	+22	+30	+19	−3	−11	+12	+39	+51		13
14			−24	−29	−40	−28	−32	−23	+1	+8	+18	+25	+42			14
15				−23	−32	−29	−26	−13	+2	+20	+24	+37				15
16					−19	−26	−16	+6	+11	+32	+36					16
17							−7	−1	+23							17
3							−16	−7	−20							3
4					0	+7	+1	+1	+7	0	−5					4
5				−1	+3	+17	−5	−4	+21	+15	+4	+9				5
6			−3	+1	+5	+35	−8	+1	−7	−1	0	−5	+10			6
7		+3	−3	0	+1	+17	−7	−3	0	−9	+5	+1	−1	+2		7
8		+1	−2	−4	−11	−39	+29	+6	−18	+28	+11	−10	−7	−1		8
9	0	−3	−9	−15	+15	+32	−19	−3	+3	+35	+4	−22	−12	−5	+16	9
10	+6	−2	−6	−3	+33	−30	−34	+32	−31	+17	−11	−23	−13	−4	+17	10
11	+7	−3	−7	−2	+19	−22	+65	−31	−45	+37	−26	−22	−4	+7	+17	11
12		−1	−4	−8	−11	+10	−26	−10	+14	+6	−14	−20	−4	+5		12
13		+2	−7	−14	−24	−6	+33	+28	−21	+1	−10	−5	+7	+13		13
14			−4	−5	−14	−1	−3	0	+12	+9	+9	+3	+9			14
15				−2	−8	−2	0	+5	−5	−6	+6	+11				15
16					0	−5	+3	+17	−6	−6	+12					16
17							+5	+4	+16							17
X (pixels)	3	4	5	6	7	8	9	10	11	12	13	14	15	16	17	*X* (pixels)
	Y (pixels)															

TABLE II

Comparison of integrated signals of the primary nucleus and its major companion, their relative position, and a mean residual from optimized solutions that involve increasing number of point sources (HST WFPC-2 image of July 25, 1996, assuming coma law A)

Number of point sources introduced	Integrated signal (ADU/s)		Major companion's		Mean residual (ADU)
	of primary nucleus, $\Im_{\rm I}$	of major companion, $\Im_{\rm II}$	separation (arcsec)	position angle	
1	792 ± 17	–	–	–	± 42.7
2	807 ± 11	145 ± 12	0.0901 ± 0.0023	$354\overset{\circ}{.}6 \pm 2\overset{\circ}{.}5$	± 31.7
4	824 ± 10	138 ± 13	0.0882 ± 0.0036	3.8 ± 1.7	± 26.2
6	822 ± 7	170 ± 8	0.0927 ± 0.0013	2.5 ± 0.8	± 20.0
8	826 ± 7	176 ± 7	0.0924 ± 0.0012	2.9 ± 0.7	± 18.3
9	829 ± 6	180 ± 7	0.0925 ± 0.0011	3.0 ± 0.6	± 17.3

a second point source into the solution improves the fit to the observed signal distribution and brings the mean residual down significantly. The results for the primary nucleus and its major companion are for the image of July 25 listed in Table II as functions of the number of point sources whose parameters were introduced as free parameters. The best solution, with nine point sources, improves the match to the observations by a factor of more than two and yields a distribution of signal residuals that is displayed in the lower panel of Table I. The pixel coordinates of the principal nucleus and its major companion are, respectively, $X = 10.42 \pm 0.01$, $Y = 9.57 \pm 0.01$ (virtually unchanged) and $X = 8.59 \pm 0.02$, $Y = 10.45 \pm 0.02$. The systematic trend of residuals across the field has disappeared, which indicates that this effect was indeed caused by neglect of the contributions from the major companion and other possible nearby objects rather than by failure of the applied coma model. The remarkable stability of the derived parameters is apparent from Table II. This is especially true for the solutions with more than four point sources, even though some of the fainter ones may in fact be artifacts of instrumental or unknown origin.

In another example, a prominent secondary peak, due to a major companion, is apparent in Figure 1, which shows a model brightness distribution for the HST image of May 20, 1996.

The primary results are summarized in Table III, after the coma contribution has been filtered out using one of two laws, A or B (Sekanina, 1997–1999). I submit that the major companions on the five exposures between May 20 and October 17, 1996 are the same object, an *orbiting satellite*. Its effective diameter is found to be equal to $\sim$33 km, derived by brightness comparison with the main nucleus (Sekanina, 1997–1999). This satellite was undetected on the image of October 23, 1995, presumably because of its subpixel separation from the principal nucleus.

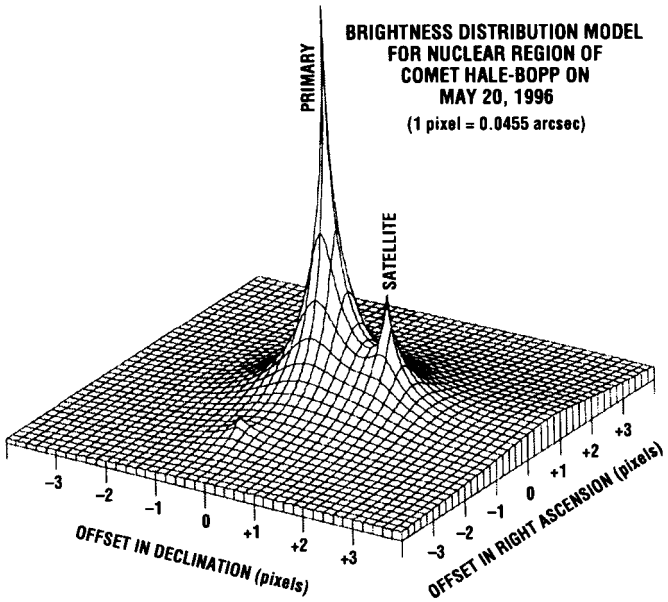

Figure 1. Model for the surface brightness distribution in the near-nucleus region derived for the image exposed on May 20, 1996. The signal of the coma was approximated by law A (Sekanina, 1997–1999). The dominant sources are the primary nucleus and its major satellite. Another, minor source is hidden behind the primary nucleus.

TABLE III

Signals and relative positions of the primary nucleus and its satellite on the HST images

Date 1996[a] (UTC)	Coma law used	Integrated signal (ADU/s) primary $\Im_I$	satellite $\Im_{II}$	ratio $\Im_{II}/\Im_I$	Satellite's separation (arcsec)	distance (km)	position angle
May 20.45	A	350 ± 7	99 ± 8	0.28 ± 0.02	0.0612 ± 0.0030	163 ± 8	351°.2 ± 2°.6
	B	402 ± 5	87 ± 6	0.22 ± 0.02	0.0970 ± 0.0023	259 ± 6	5.8 ± 1.2
June 22.49	A	688 ± 8	136 ± 8	0.20 ± 0.01	0.0965 ± 0.0019	211 ± 4	314.0 ± 1.1
	B	689 ± 8	131 ± 9	0.19 ± 0.01	0.0951 ± 0.0023	208 ± 5	314.4 ± 1.3
July 25.60	A	829 ± 6	180 ± 7	0.22 ± 0.01	0.0925 ± 0.0011	184 ± 2	3.0 ± 0.6
	B	819 ± 7	164 ± 7	0.20 ± 0.01	0.0920 ± 0.0014	183 ± 3	3.1 ± 0.8
Sept. 23.18	A[b]	827 ± 12	169 ± 15	0.20 ± 0.02	0.0751 ± 0.0025	161 ± 5	1.5 ± 1.9
	B	838 ± 23	191 ± 23	0.23 ± 0.03	0.0786 ± 0.0036	168 ± 8	359.1 ± 2.6
Oct. 17.63	A	521 ± 9	83 ± 11	0.16 ± 0.02	0.0872 ± 0.0040	192 ± 9	58.7 ± 1.5
	B	370 ± 21	65 ± 9	0.18 ± 0.03	0.1542 ± 0.0057	340 ± 13	53.9 ± 1.8

[a] On October 23.27, 1995 the satellite was not detected, probably because of subpixel separation from primary; $\Im_I$ (or $\Im_I + \Im_{II}$) is 55 ± 1 ADU/s with law A and 56 ± 1 ADU/s with law B.

[b] An alternative, but less probable candidate has entries in columns 4–8: 215±12 ADU/s, 0.26±0.02, 0.0828 ± 0.0015 arcsec, 177 ± 3 km, and 131°.7 ± 1°.1.

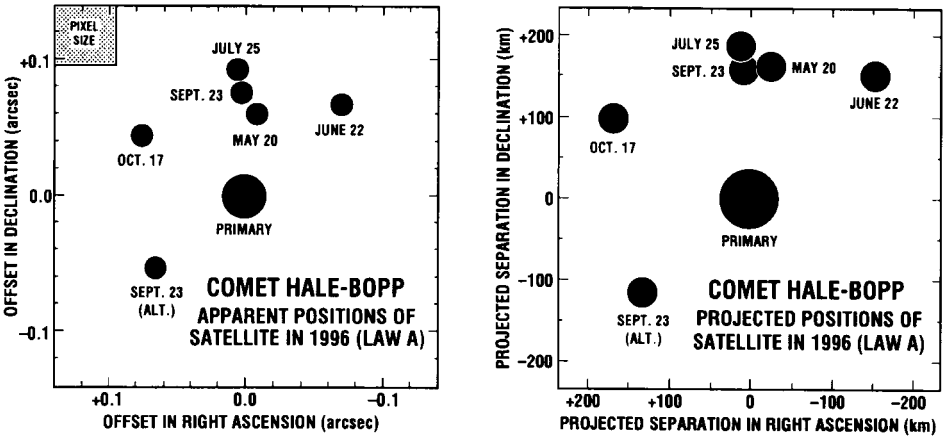

Figure 2. The satellite's apparent offsets (on the left) and projected separation distances (on the right) from the principal nucleus on five dates in 1996 have been derived from the optimized solutions with law A for the coma. In either panel, the dimensions of the main nucleus (∼70 km across) and the satellite (∼30 km across) are drawn to scale. To avoid collision, the separation distance must exceed 50–60 km (or more for irregularly shaped objects) at all times. Notice an alternative candidate for the satellite on September 23. The pixel size is shown as a shaded square in the upper left corner of the left-hand side panel.

The results are relatively insensitive to the coma law used, even though law B, leaving higher formal errors on the average, leads to wider separations in May and October 1996. For September 23, the solution based on law A offers for the satellite two candidates in different directions from the principal nucleus.

Figure 2 shows the satellite's separations from the principal nucleus, with the sizes of both objects drawn to scale. The prevalence of the offsets to the north may be a signature of an elongated orbit's apoapsis, near which the satellite should spend most of the time. I find no strong correlation with the directions of persistent dust jets as listed by Boehnhardt et al. (1999).

3. Dynamical Stability of the Comet Pair and Its Orbital Period

Given the separation distances in Table III, the system's dynamical stability is obviously of major concern. In Laplace's classical definition, the boundary of a body's gravitational sphere of action is the surface on which the force of gravity of this central body expressed in units of the disturbing force of the perturbing body equals the force of gravity of the perturbing body expressed in units of the disturbing force of the central body. Identifying the central body with the principal nucleus and the perturbing body with the Sun, and considering that the dimensions of the comet's sphere of action are orders of magnitude smaller than the distance

Sun–comet, the following expression is found for radius r_0 (in km) of the sphere of action of the principal nucleus:

$$r_0 = 6.24 \times 10^{-6}\, r_\odot\, M_{\rm I}^{2/5}, \tag{1}$$

where $r_\odot$ is the comet's heliocentric distance (in AU) and $M_{\rm I}$ is the mass of the principal nucleus (in g). The radius of the Earth's sphere of action is 805,000 km, almost exactly twice the Moon's distance at apogee.

With a bulk density of 0.2–0.5 g/cm^3, one gets for the nucleus of $\sim$70 km in diameter (Sekanina, 1999) $M_{\rm I}$ = (3.4–8.6) $\times$ 10^{19} g and r_0 = 370–540 km at perihelion (0.914 AU) and $>$1000 km at heliocentric distances exceeding $\sim$2–3 AU; at $\sim$180 km, the satellite should be in a fairly stable orbit even at perihelion. The escape velocity is 12–19 m/s at the primary's surface, but only 5–8 m/s at a distance of 180 km. On the other hand, with Weaver et al.'s (1997) estimate of $\leq$42 km for the primary's diameter, r_0 is always $<$300 km at perihelion and the satellite's orbit should then become unstable.

The orbital period P (in days) of a satellite of mass $M_{\rm II}$ which moves at an average distance of S (in km) from the primary of mass $M_{\rm I}$ (in g) is

$$P = 8.92 \times 10^6\, S^{3/2}\, [M_{\rm I}(1+\mu)]^{-1/2}\,, \tag{2}$$

where $\mu = M_{\rm II}/M_{\rm I}$. From the signal ratio $\Im_{\rm II}/\Im_{\rm I}$ (Table III) I estimate that $\mu \simeq 0.1$. At an average distance of $S \simeq 180$ km (assuming no foreshortening), the orbital period is 2–3 days if the primary is $\sim$70 km across, but 9–15 days if it is 27 km in diameter, equal to Weaver et al.'s lower limit for the size. In either case, the period is much shorter than the 1–2 month intervals between two consecutive HST observations. While this circumstance will complicate the satellite's orbit determination and the finding of the total mass for the system, there are plans to get the project under way in the near future.

4. Supporting Evidence and Relevant Constraints

Two independent reports support and strengthen evidence for the existence of a second mass in close proximity to the principal nucleus. Based on their observations made with the ADONIS adaptive optics system mounted on the 3.6-meter telescope at ESO La Silla, Marchis et al. (1999) are reporting the central brightness peak in the coma to have been double on November 6, 1997 and again on January 15, 1998, with separations of 0.2–0.4 arcsec. Beuzit (Rigaut and Beuzit, 1997) has remarked that, on September 30, 1996 (only one week after a set of images was taken with the HST), a knot of material 0.15 arcsec north of the nucleus was detected on images obtained with a PUEO adaptive optics system installed on the CFHT 3.6-meter telescope at Mauna Kea.

The existence of an orbiting satellite is attractive conceptually, because it could account for the comet's enormous brightness and complex dust-coma morphology as products of overlapping activity from the two objects. Two active nuclei are implied by detailed analysis of the system of dust halos widely observed in early 1997. Sekanina (1998) has concluded that the halo system in the *southeastern* quadrant in late February could not be explained by dust ejecta from any location on the nucleus that was the source of the periodically recurring bright jets and halos in the *southwestern* quadrant. Sekanina's binary concept is also suggested by Vasundhara and Chakraborty (1999) as a solution to problems encountered by their morphological model.

Perhaps the most controversial aspect of the problem of nuclear duplicity is the apparent absence of the satellite nucleus on the HST images. At present, quantitative comments can only be made on the images taken on the five days between May 20 and October 17, 1996, on which the satellite was digitally detected. In each of these cases, the separation distance between the principal nucleus and the satellite was close to 2 pixels and their signal ratio approximately 5 : 1. It is straightforward to show that, given this separation distance, this signal ratio, and the shape of the point spread function (PSF) for the planetary mode of the WFPC-2, the satellite indeed could not be visually resolved. If one superimposes the PSFs of the two objects, he finds that the satellite could show only as a "shoulder" on the slope of the PSF of the principal nucleus. At a separation distance of 2 pixels, the pair can visually be resolved into two distinct masses only when the signal ratio is confined to between 1 : 1 and $\sim$3 : 1. Thus, the failure to detect the satellite by visually inspecting the 1996 HST images cannot be construed as an argument against the satellite's existence. A similar extrapolation may likewise be inadmissible for the post-perihelion HST images taken with the STIS instrument and reproduced by Weaver and Lamy (1999).

Acknowledgements

I thank Hermann Boehnhardt for directing my attention to J.-L. Beuzit's electronic report. I am grateful to Harold A. Weaver for providing me with the HST digital charts of the near-nucleus region; for information on the HST image calibration; and for his helpful critique. This work is based on observations made with the NASA/ESA Hubble Space Telescope obtained at the Space Telescope Science Institute, which is operated by the Association of Universities for Research in Astronomy, Inc., under contract with the National Aeronautics and Space Administration. This research was carried out at the Jet Propulsion Laboratory, California Institute of Technology, under contract with the National Aeronautics and Space Administration.

References

Boehnhardt, H., Birkle, K., Colas, F., Fiedler, A., Jorda, L., Peschke, S., Rauer, H., Schulz, R., Schwehm, G., Thomas, N., Tozzi, G., and West, R. M.: 1997–1999, *Earth, Moon, and Planets* **78**, in press.

Marchis, F., Boehnhardt, H., Hainaut, O., and Le Mignant, D.: 1999, *Astron. Astrophys.*, in press.

Rigaut, F. and Beuzit, J.-L.: 1997, Electronic report updated on March 11, 1997 (URL http://www.cfht.hawaii.edu/manuals/aob/best_pictures.html).

Sekanina, Z.: 1995, *Astron. Astrophys.* **304**, 296–316.

Sekanina, Z.: 1997–1999, this issue.

Sekanina, Z.: 1998, *Astrophys. J.* **509**, L133–L136.

Vasundhara, R. and Chakraborty, P.: 1999, *Icarus*, in press.

Weaver, H. A., Feldman, P. D., A'Hearn, M. F., Arpigny, C., Brandt, J. C., Festou, M. C., Haken, M., McPhate, J. B., Stern, S. A., and Tozzi, G. P.: 1997, *Science* **275**, 1900–1904.

Weaver, H. A. and Lamy, P. L.: 1997–1999, *Earth, Moon, and Planets* **79**, in press.